Supplementary Material

for

Efficient removal of antibiotic ciprofloxacin by catalytic wet air oxidation using sewage sludge-based catalysts. Degradation mechanism by DFT studies.

Pablo Gutiérrez-Sánchez[1*], Silvia Álvarez-Torrellas[1], Marcos Larriba[1], M. Victoria Gil[2], Juan M. Garrido-Zoido[2], Juan García[1*]

[1]*Catalysis and Separation Processes Group, Chemical Engineering and Materials Department, Faculty of Chemistry, Complutense University, Avda. Complutense s/n, 28040, Madrid, Spain.*
[2]*Departamento de Química Orgánica e Inorgánica, Facultad de Ciencias and IACYS Unidad de Química Verde y Desarrollo Sostenible, Universidad de Extremadura, E-06006 Badajoz, Spain***.**

Corresponding author
E-mail address: pgutie03@ucm.es; jgarciar@ucm.es; +34 91394.5207

Tables: 5

Figures: 10

Table S1. Comparison of several advanced oxidation processes in the ciprofloxacin removal.

Process	Reference	Year	$C_{0\ Ciprofloxacin}$ (mg/L)	Degradation (%)	t (min)	Conditions
Photocatalysis	[1]	2022	10	93.5	60	Light intensity = 100 mW/cm^2 , power of 300 W, Co_3O_4/SiNWs-30/PMS, C_{PMS} = 0.52 mM, pH = 7
Cavitation	[2]	2022	10-100	79-95	180	ΔP = 0.5, 1, 1.5, and 2 bar, CIP: H_2O_2= 1:100, 1:300, 1:500, 1:700, 1:1000, and 1:1500, pH = 6.6–7.8
Photocatalysis	[3]	2022	20-40	96.1	30	Cu-doped Bi_2S_3, Xe lamp, light intensity = 50 mW/cm^2, 5.0 < pH < 9.0
Heterogeneous Fenton	[4]	2019	10	80-90	20-4h	[sludge biochar catalyst] = 0.2 g·L^{-1}, pH = 4, [H_2O_2] = 10mM
Fenton´s oxidation	[5]	2018	100	70	60	[H_2O_2]:[Fe^{2+}] = 10, stoichiometric [H_2O_2] = 14.2 mM and initial wastewater pH = 3
Fenton	[6]	2013	50	90	30	pH = 2, [H_2O_2]:[Fe^{2+}] = 2.7
This work		2022	50	99	180	T = 140ºC, P = 20 bar, m_{cat} = 0.7 g/L, pH_0=7

Table S2. Cartesian coordinates for optimized structure of ciprofloxacin.

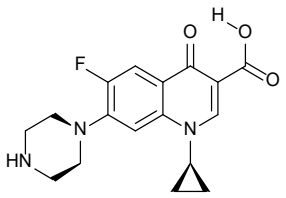

ATOM TYPE	x	y	z
C	1.16925600	-2.03831100	-0.26296700
C	1.75749000	-0.76374200	-0.47890100
C	0.87998700	0.31577300	-0.51864800
C	-0.49212900	0.15086700	-0.31653400
C	-1.03204200	-1.12043400	-0.07685900
C	-0.16029100	-2.22005900	-0.06067400
N	-1.34375100	1.25777000	-0.33905500
C	-2.65729100	1.09457900	-0.18713000
C	-3.25161800	-0.12269300	0.03177100
C	-2.45308500	-1.30839200	0.11247600
F	1.95403100	-3.12726200	-0.33012100
C	-0.79725400	2.58229400	-0.57850700
C	0.03892900	3.21753500	0.48298700
C	-1.33521100	3.74142800	0.18790700
O	-2.95126500	-2.44343900	0.32749200
C	-4.71699500	-0.17185700	0.19026300
O	-5.22297900	-1.37802100	0.41269800
O	-5.43846600	0.80595300	0.12587300
N	3.11448300	-0.65341600	-0.72171600
C	4.04515700	-1.28070100	0.23641900
C	4.32906400	-0.34967600	1.40247400
N	4.90591400	0.90404800	0.91601500
C	3.95024300	1.56535400	0.02455700
C	3.64441200	0.64523800	-1.14729400
H	1.26456800	1.30477900	-0.69267400
H	-0.54831100	-3.21933300	0.07844000
H	-3.25844300	1.99067100	-0.24377100
H	-0.50883200	2.73477400	-1.60879300
H	0.90045200	3.78059200	0.15683600
H	0.16300100	2.66027500	1.40063000
H	-2.10061500	3.54878400	0.92511900
H	-1.43473600	4.67144200	-0.34983500
H	-4.45300900	-2.03276400	0.42691900
H	3.64037700	-2.21481200	0.60500500
H	4.97108600	-1.49576300	-0.29842100
H	3.39091100	-0.17993800	1.94947200
H	5.03065200	-0.83263600	2.08067700
H	5.07192900	1.50957800	1.71114500
H	4.38359600	2.48992900	-0.35314200
H	3.02215000	1.81907400	0.55234400
H	4.57353300	0.44161100	-1.68183000
H	2.95883800	1.11110400	-1.85028500

Table S3. Cartesian coordinates for optimized structure of intermediate 1.

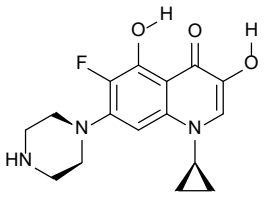

ATOM TYPE	x	y	z
C	0.73348600	-1.90742900	-0.26252700
C	1.31937500	-0.64034400	-0.49130300
C	0.46978700	0.46070800	-0.51492800
C	-0.90435000	0.31943100	-0.28524800
C	-1.46502400	-0.94949800	-0.03562800
C	-0.60411900	-2.07535100	-0.03390600
N	-1.73930900	1.41675000	-0.28393400
C	-3.07720200	1.26986300	-0.10162400
C	-3.65611400	0.06430100	0.12113400
C	-2.86990000	-1.12269900	0.17443000
F	1.48581200	-3.02112700	-0.34820500
C	-1.20012400	2.73643400	-0.54396600
C	-0.31645400	3.37102900	0.48012400
C	-1.70201900	3.89564600	0.24825000
O	-3.41567900	-2.24547400	0.38964600
N	2.68018000	-0.55943300	-0.75585000
C	3.60236900	-1.19230600	0.20649500
C	3.90754100	-0.25838700	1.36456200
N	4.50870400	0.97920500	0.86573900
C	3.56218800	1.65204700	-0.02730600
C	3.22932700	0.72838800	-1.18935700
H	0.87135400	1.44149200	-0.69138800
H	-3.66864500	2.17226800	-0.14234200
H	-0.95609300	2.89838000	-1.58498500
H	0.52900400	3.93656200	0.11783500
H	-0.14996200	2.81142300	1.38955800
H	-2.43477700	3.69914700	1.01698200
H	-1.82470900	4.82838900	-0.28009100
H	3.18283900	-2.11670900	0.58350300
H	4.52380300	-1.42857300	-0.32766900
H	2.97448100	-0.06443000	1.91240900
H	4.60072500	-0.74941300	2.04571000
H	4.68970200	1.58784400	1.65520500
H	4.01360500	2.56330900	-0.41639100
H	2.64355400	1.93107800	0.50357800
H	4.15069600	0.50687900	-1.73065200
H	2.54604600	1.20313100	-1.88863700
O	-5.00671700	-0.03736700	0.30524600
H	-5.19929000	-0.97540800	0.45307200
O	-1.09193400	-3.31864600	0.15415200
H	-2.06962400	-3.20998900	0.28890300

Table S4. Cartesian coordinates for optimized structure of intermediate 2.

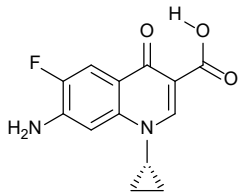

ATOM TYPE	x	y	z
C	-2.70244000	-1.41001800	0.05153800
C	-3.01505200	-0.04384100	-0.11678400
C	-1.95805200	0.85040000	-0.21631000
C	-0.64030400	0.39823100	-0.14318900
C	-0.35825400	-0.97024800	0.01808700
C	-1.43102300	-1.87379500	0.11656300
N	0.42106700	1.30015000	-0.24170000
C	1.67953300	0.86198600	-0.22561600
C	2.02268300	-0.45735500	-0.07655900
C	1.00213200	-1.45262600	0.06703300
F	-3.74207900	-2.25817300	0.14064300
C	0.14493600	2.71484200	-0.42018100
C	-0.40365800	3.49064200	0.73096400
C	1.00574000	3.71621100	0.26947400
O	1.27185100	-2.67324600	0.21872000
C	3.45315300	-0.81597000	-0.06208000
O	3.71244900	-2.10684700	0.10057300
O	4.35584400	-0.00897700	-0.18623900
N	-4.31671100	0.35184000	-0.13073700
H	-2.18207900	1.89705600	-0.35302100
H	-1.24325000	-2.93106600	0.23898800
H	2.44560200	1.61518100	-0.33888600
H	-0.22441400	2.94605900	-1.40916100
H	-1.15664800	4.23143300	0.50899900
H	-0.53300200	2.95358200	1.65961500
H	1.79424700	3.34854800	0.90937400
H	1.23798600	4.61478000	-0.28069700
H	2.82622400	-2.58739200	0.18097700
H	-4.51415200	1.27807900	-0.47622600
H	-5.01980200	-0.34481800	-0.32075300

Table S5. Energetic data of organic compounds involved in the reaction and caffeine as reference.

Compound	Electronic energies (kcal/mol)	Sum of electronic and thermal free energies (kcal/mol)	Entropy (cal/(mol·K))	Electronic energies (Hartrees)	Energies HOMO (eV)	Energies LUMO (eV)
Ciprofloxacin	-720626.16	-720458.36	168.55	-1148.39	-7.22	-0.98
Intermediate 1	-696697.04	-696532.03	164.74	-1110.26	-6.88	-0.75
Intermediate 2	-587998.39	-587895.96	142.78	-937.03	-7.56	-0.94
Formaldehyde	-71848.12	-71848.53	50.54	-114.50	-9.48	-0.10
Formic acid	-119082.05	-119080.54	57.32	-189.77	-10.35	0.39
Acetic acid	-143755.36	-143739.38	68.55	-229.09	-10.06	0.14
Oxalic acid	-237418.40	-237412.27	75.94	-378.35	-10.17	-1.02
Caffeine	-426934.64	-426851.11	123.26	-680.36	-7.61	-0.15

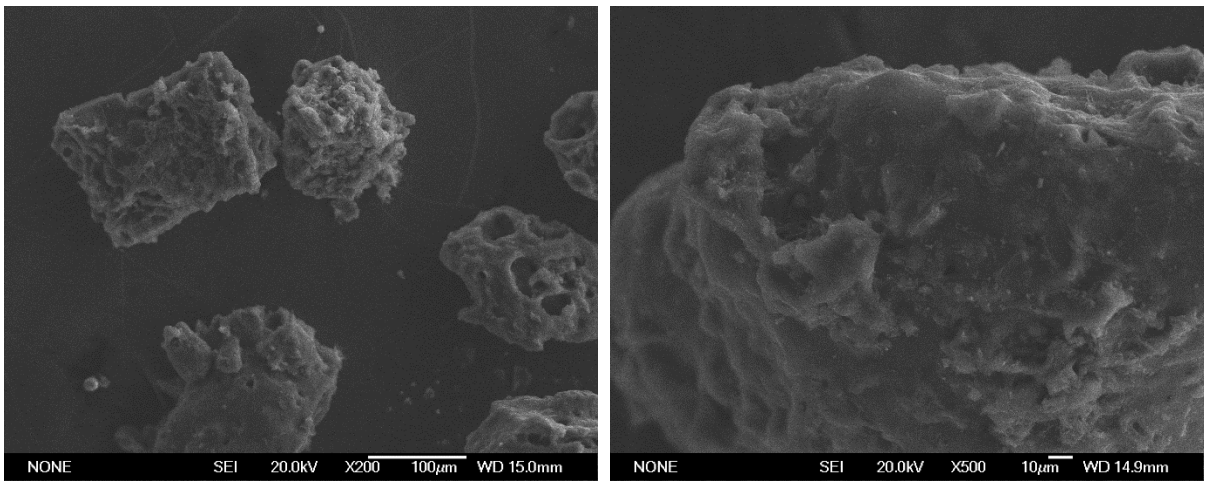

Figure S1. SEM micrographs of the FeSAC catalyst with different magnification.

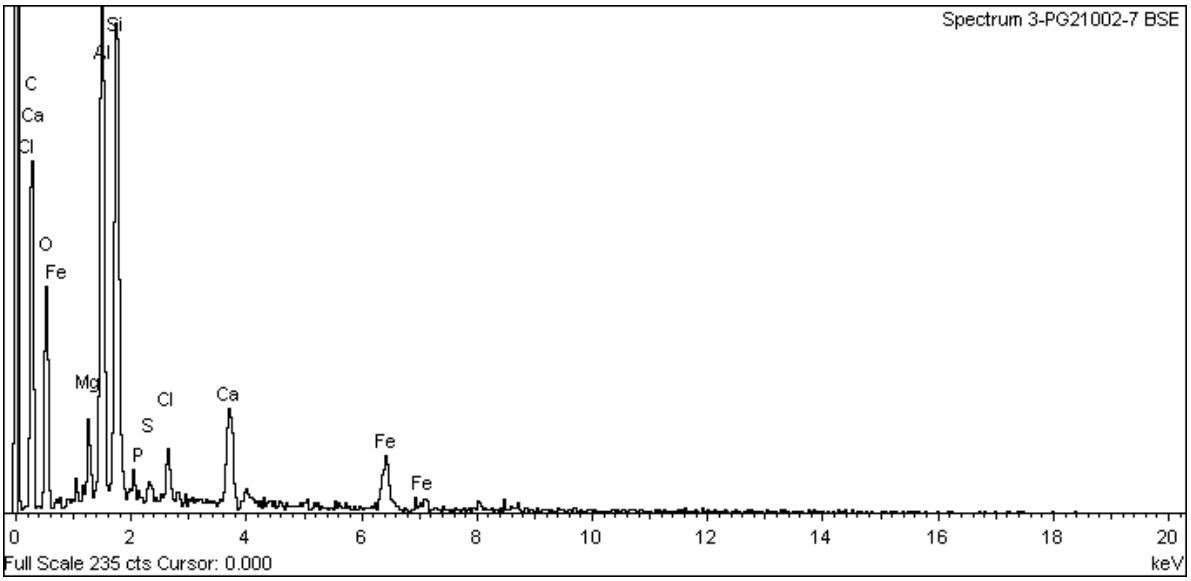

Figure S2. EDX analysis of FeSAC catalyst.

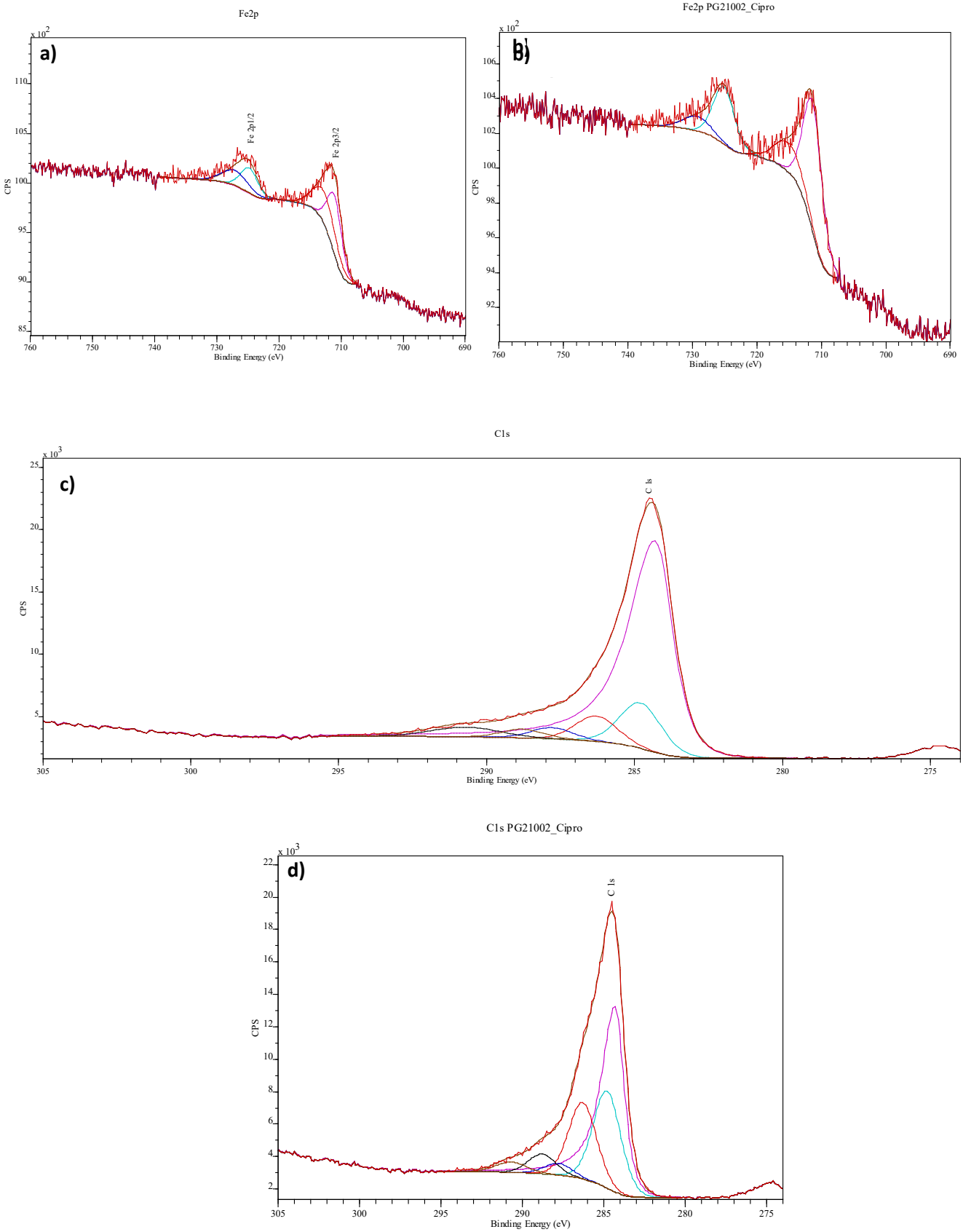

Figure S3. Fe2p, C1s and O1s deconvoluted XPS spectrum of fresh catalyst as prepared (a, c, e) and after used in experiment (b, d, f), respectively.

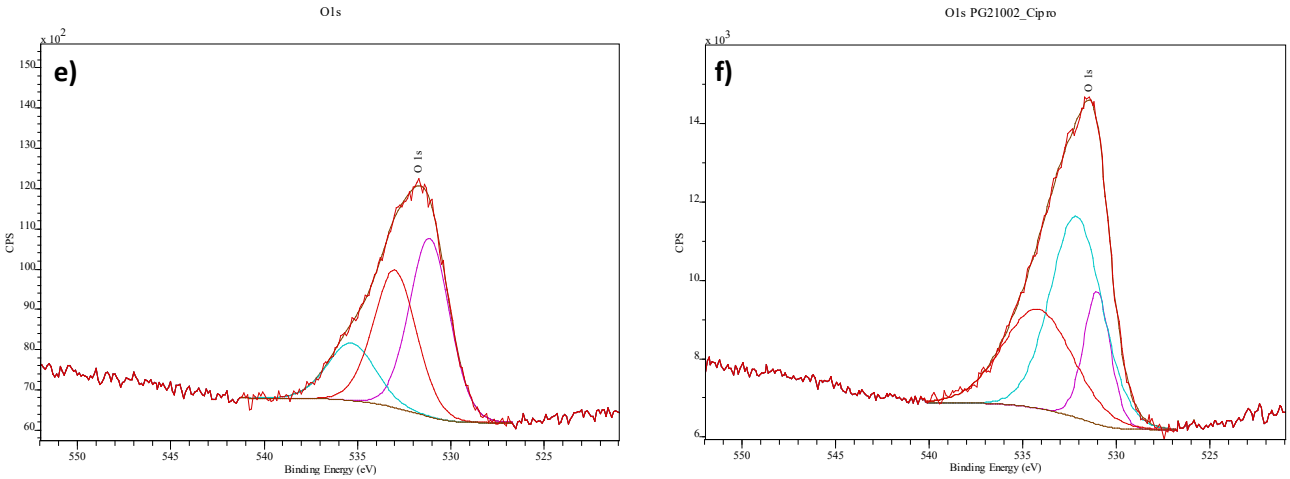

Figure S3. (cont.) Fe2p, C1s and O1s deconvoluted XPS spectrum of fresh catalyst as prepared (a, c, e) and after used in experiment (b, d, f), respectively.

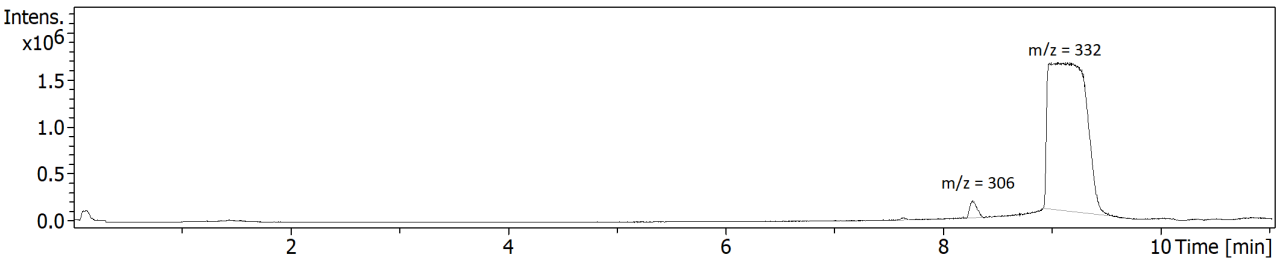

Figure S4. LC-MS chromatogram for the liquid sample at zero time from CWAO reaction.

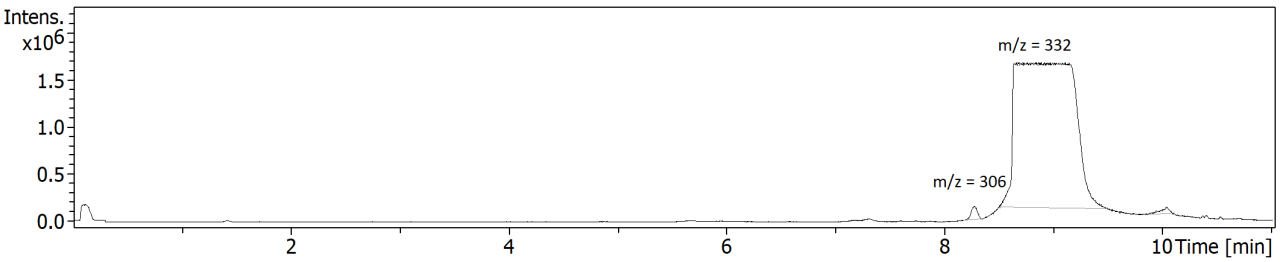

Figure S5. LC-MS chromatogram for the initial ciprofloxacin solution at 50 mg/L.

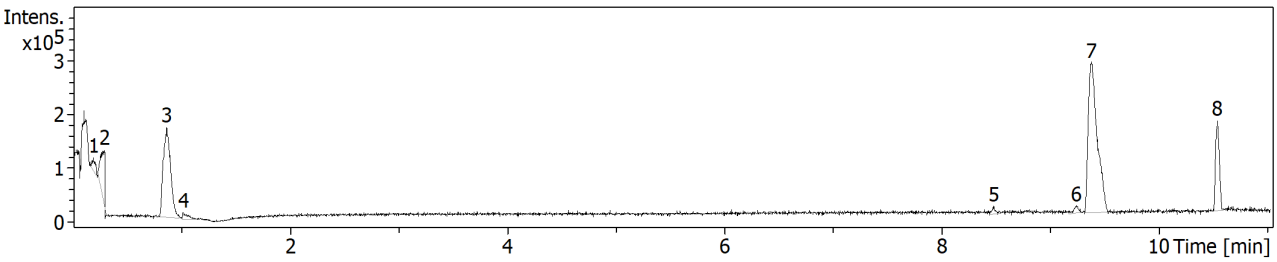

Figure S6. LC-MS chromatogram for the liquid sample after a reaction time of 180 min.

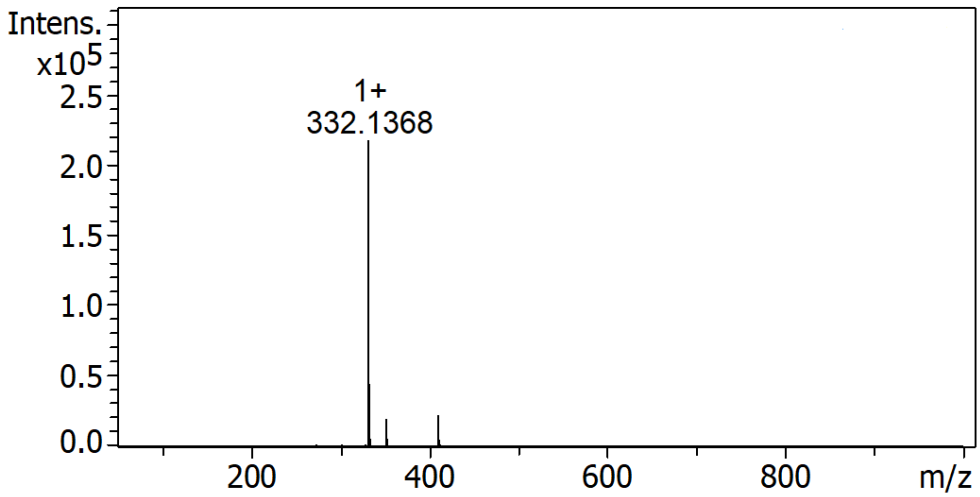

Figure S7. Mass spectrum of ciprofloxacin solution at t_R=9.4 min.

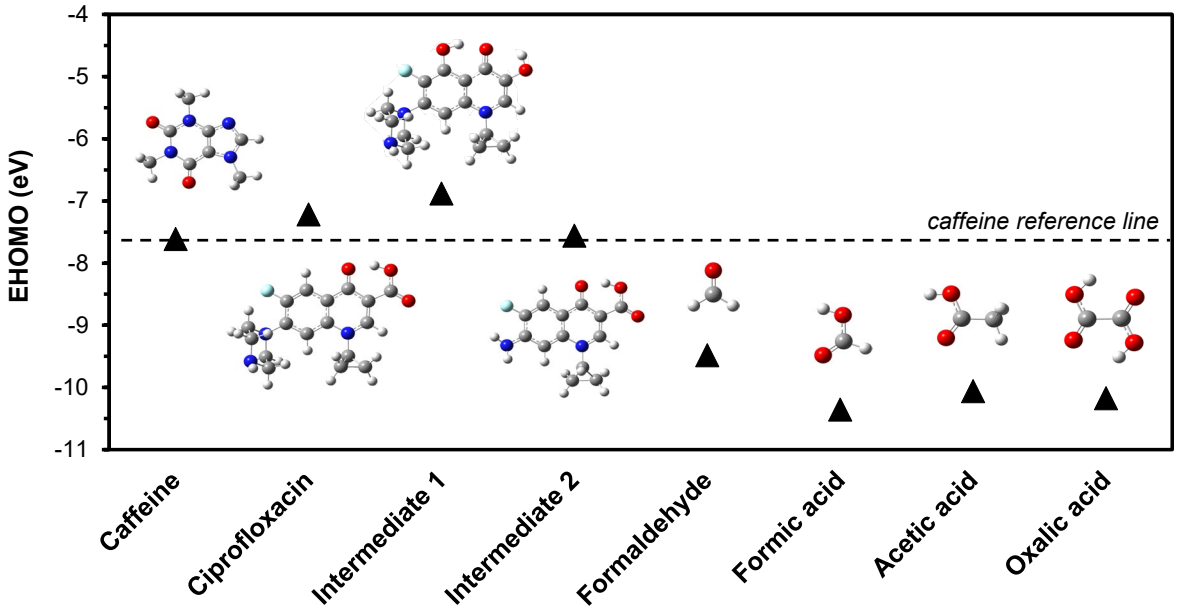

Figure S8. E_{HOMO} (eV) comparative diagram of ciprofloxacin, intermediates, and final products (caffeine as reference).

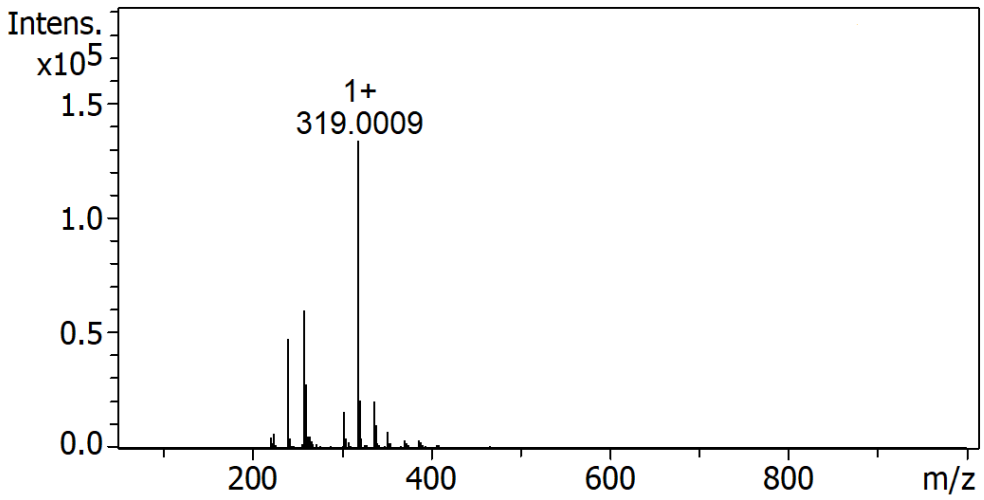

Figure S9. Mass spectrum of ciprofloxacin solution at t_R=0.9 min.

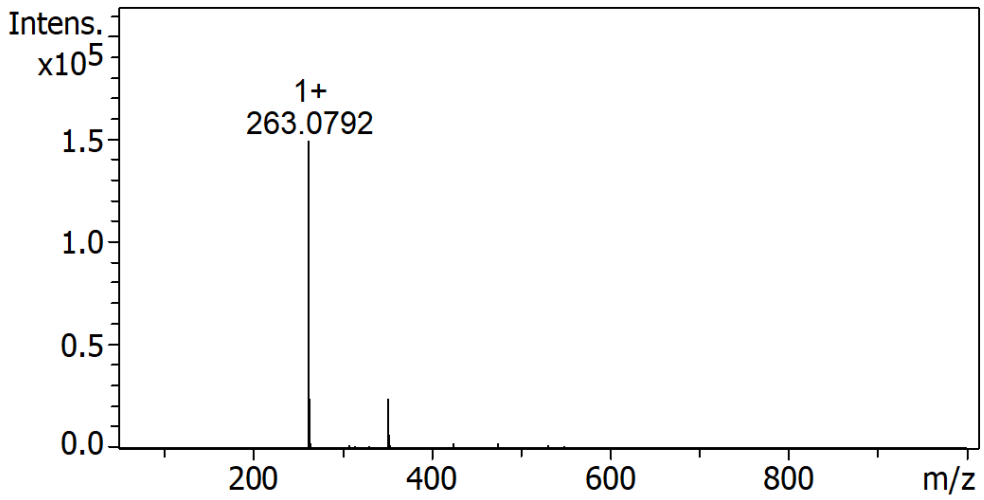

Figure S10. Mass spectrum of ciprofloxacin solution at t_R=10.5 min.

References:

[1] L. Yao, X. He, J. Lv, G. Xu, Z. Bao, J. Cui, D. Yu, Y. Wu, Efficient degradation of ciprofloxacin by Co_3O_4/Si nanoarrays heterojunction activated peroxymonosulfate under simulated sunlight: Performance and mechanism, J. Environ. Chem. Eng. 10 (2022) 107397.

[2] P.B. Patil, P. Thanekar, V.M. Bhandari, Intensified hydrodynamic cavitation using vortex flow based cavitating device for degradation of ciprofloxacin, Chem. Eng. Res. Des. 187 (2022) 623-632.

[3] F. Du, Z. Lai, H. Tang, H. Wang, C. Zhao, Construction and application of BiOCl/Cu-doped Bi_2S_3 composites for highly efficient photocatalytic degradation of ciprofloxacin, Chemosphere 287 (2022) 132391.

[4] J. Li, L. Pan, G. Yu, S. Xie, C. Li, D. Lai, et al., The synthesis of heterogeneous Fenton-like catalyst using sewage sludge biochar and its application for ciprofloxacin degradation, Sci. Total Environ. 654 (2019) 1284–1292.

[5] A. Gupta, A. Garg, Degradation of ciprofloxacin using Fenton's oxidation: Effect of operating parameters, identification of oxidized by-products and toxicity assessment, Chemosphere 193 (2018) 1181–1188.

[6] J. F. Yang, H. H. Chen, Degradation of Ciprofloxacin in Aqueous Solution by the Fenton Process', Adv. Mater. Res. 610–613 (2012) 352–355.